0026-895X/10/7804-693–703$20.00
MOLECULAR PHARMACOLOGY
Vol. 78, No. 4
65839/3625342
*Mol Pharmacol* 78:693–703, 2010
*Printed in U.S.A.*




# Mechanism-Based Inactivation of Cytochrome P450 3A4 by Lapatinib[S]

Woon Chien Teng, Jing Wen Oh, Lee Sun New, Michelle D. Wahlin, Sidney D. Nelson, Han Kiat Ho, and Eric Chun Yong Chan

*Department of Pharmacy, Faculty of Science, National University of Singapore, Singapore (W.C.T., J.W.O, L.S.N, H.K.H., E.C.Y.C.); Department of Medicinal Chemistry, University of Washington, Seattle, Washington (M.D.W., S.D.N.); and Institute of Medical Biology, Agency for Science, Technology and Research, Singapore (H.K.H.)*

Received April 25, 2010; accepted July 6, 2010

## ABSTRACT

Fatalities stemming from hepatotoxicity associated with the clinical use of lapatinib (Tykerb), an oral dual tyrosine kinase inhibitor (ErbB-1 and ErbB-2) used in the treatment of metastatic breast cancer, have been reported. We investigated the inhibition of CYP3A4 by lapatinib as a possible cause of its idiosyncratic toxicity. Inhibition of CYP3A4 was time-, concentration-, and NADPH-dependent, with $k_{inact} = 0.0202\ min^{-1}$ and $K_i = 1.709\ \mu M$. The partition ratio was approximately 50.9. Addition of GSH did not affect the rate of inactivation. Testosterone protected CYP3A4 from inactivation by lapatinib. The characteristic Soret peak associated with a metabolite-intermediate complex was not observed for lapatinib during spectral difference scanning. However, reduced carbon monoxide (CO)-difference spectroscopy did reveal a 43% loss of the spectrally detectable CYP3A4-CO complex in the presence of lapatinib. Incubation of either lapatinib or its dealkylated metabolite with human liver microsomes in the presence of GSH resulted in the formation of a reactive metabolite (RM)-GSH adduct derived from the O-dealkylated metabolite of lapatinib. In addition, coincubation of lapatinib with ketoconazole inhibited the formation of the RM-GSH adduct. In conclusion, we demonstrated for the first time that lapatinib is a mechanism-based inactivator of CYP3A4, most likely via the formation and further oxidation of its O-dealkylated metabolite to a quinoneimine that covalently modifies the CYP3A4 apoprotein and/or heme moiety.





## Introduction

Lapatinib (Fig. 1), the first oral dual tyrosine kinase inhibitor of ErbB-1 and ErbB-2, was approved by the US Food and Drug Administration in 2007. As a targeted therapy that inhibits the tyrosine kinase domains on ErbB-1 and ErbB-2, it inhibits downstream cell proliferation and induces apoptosis by the extracellular signal-regulated kinase-1/2 and phosphatidylinositol 3-kinase/Akt pathways, respectively (Rusnak et al., 2001; Xia et al., 2002). Lapatinib is usually indicated for coadministration with capecitabine in those patients having the subtype of advanced metastatic breast cancer in which there is ErbB-2 overexpression and resistance to standard therapy such as anthracyclines (e.g., doxorubicin) and taxane (Medina and Goodin, 2008). Both in vitro and in vivo data further demonstrated the effectiveness of lapatinib even in cases resistant to trastuzumab, the first therapeutic monoclonal antibody directed against ErbB-2 (Ryan et al., 2008). The potential of lapatinib's efficacy in metastatic breast cancer has also been demonstrated in various trials (Nelson and Dolder, 2007). Hence, lapatinib presents itself as a promising alternative and orally available drug for the disease.

However, a black-boxed warning for lapatinib-related hepatotoxicity was released after postmarketing surveillance and clinical trial reports on elevated liver enzymes and rare

This work was supported by the National University of Singapore (NUS) [Grants *R*-148-000-100-112, R-279-000-249-646, *R*-148-000-117-133]; the NUS Department of Pharmacy [Final Year Project Grant *R*-148-000-003-001]; and the Biomedical Research Council, Agency for Science, Technology, and Research.

Article, publication date, and citation information can be found at http://molpharm.aspetjournals.org.

doi:10.1124/mol.110.065839.

[S] The online version of this article (available at http://molpharm.aspetjournals.org) contains supplemental material.

**ABBREVIATIONS:** P450, cytochrome P450; MBI, mechanism-based inactivator; RM, reactive metabolite; ACN, acetonitrile; HLM, human liver microsome; LC/MS/MS, liquid chromatography/tandem mass spectrometry; $K_i$, inactivator concentration at half-maximum rate of inactivation; $k_{inact}$, inactivation rate constant at infinite inactivator concentration; $K_{obs}$, observed inactivation rate constant; DMSO, dimethyl sulfoxide; ESI, electrospray ionization; EP, entrance potential; CE, collision energy; CXP, collision cell exit potential; QTOFMS, quadrupole, orthogonal acceleration time-of-flight tandem mass spectrometer; IDR, idiosyncratic drug reaction; MIC, metabolite-intermediate complex; LAPA, lapatinib; i-FIT, the likelihood that the isotopic pattern of the elemental composition matches a cluster of peaks in the spectrum.

cases of liver-related deaths (Gomez et al., 2008). Fatalities stemming from hepatotoxicity associated with its clinical use were also reported (European Medicines Agency, 2008). Because the hepatotoxicity of lapatinib has occurred in small numbers of patients and develops several days to months after commencement of therapy, it seems to be idiosyncratic in nature. To date, the mechanism by which lapatinib causes hepatotoxicity is unknown.

Lapatinib is extensively metabolized by cytochrome P450 (P450) enzymes, in particular CYP3A4/5 and, to a lesser extent, CYP2C8 (European Medicines Agency, 2008). Our in-house studies demonstrated that lapatinib is metabolized to form O- and N-dealkylated metabolites M1 and M2, respectively (Fig. 1). Specifically, the structure of O-dealkylated lapatinib has the potential to generate a reactive quinoneimine similar to the model hepatotoxin acetaminophen (Hinson et al., 1981; Dhalin et al., 1984 ). Quinoneimines are electrophilic and have the propensity to react with nucleophilic groups of cellular proteins, leading to toxicities. In fact, such bioactivation of drugs to electrophilic reactive species in inducing organ-directed toxicity is one of the most common causes for drug withdrawal (Park et al., 2006). These electrophilic species may bring about direct covalent modification of hepatic proteins to cause cellular dysfunction, or may form haptens, which in turn trigger an immune response, resulting in hepatotoxicity (Masubuchi and Horie, 2007). Lapatinib has been shown to be a strong inhibitor of CYP3A4 (GlaxoSmithKine, 2007). This information, coupled with its structural predisposition for metabolic activation and reactivity, led us to hypothesize that lapatinib undergoes biotransformation to form reactive electrophilic species that inhibit CYP3A4 irreversibly via mechanism-based inactivation.

CYP3A4 is the most abundant isoform of the P450 superfamily in humans. It has broad substrate specificity, and approximately 60% of xenobiotics are metabolized by CYP3A4. Mechanism-based inactivation of CYP3A4 may lead to accumulation of coadministered drugs in clinical practice, resulting in unforeseen toxicity (Lin et al., 2002). The number of drugs that have been characterized as mechanism-based inactivators (MBIs) has been increasing because of our greater understanding of its clinical importance. There are several criteria used in the characterization of MBIs: time-dependence of inactivation, saturable kinetics of inactivation with respect to inhibitor concentration, inactivation in a catalytically competent system, substrate protection of enzyme from inactivation, lack of suppression of inactivation by exogenous nucleophiles, irreversibility of inactivation, and 1:1 binding stoichiometry of inactivator to inactivated enzyme (Rock et al., 2009).

In this study, the nature of CYP3A4 inhibition by lapatinib was investigated based on the criteria in characterizing MBIs. GSH-trapping experiments were also performed to trace the formation of electrophilic reactive metabolites (RMs) of lapatinib that might contribute to any observed covalent modification of CYP3A4. Our results confirmed the generation of an electrophilic RM by lapatinib and established for the first time that lapatinib is a potent MBI of CYP3A4, most likely through oxidation of its O-dealkylated metabolite to a quinoneimine.

## Materials and Methods

**Chemicals.** High-performance liquid chromatography-grade methanol and acetonitrile (ACN) were purchased from Tedia Company Inc. (Fairfield, OH). Lapatinib was purchased from LC Laboratories (Woburn, MA). GSH, verapamil hydrochloride, ketoconazole, erythromycin, amodiaquine dihydrochloride, quercetin dihydrate, Tergitol NP-40, and Safranin O were purchased from Sigma-Aldrich (St. Louis, MO). Testosterone was purchased from Merck (Darmstadt, Germany). Gemfibrozil glucuronide was purchased from Toronto Research Chemicals Inc (Toronto, ON, Canada). Human recombinant P450 3A4 and 2C8 supersomes (rCYP3A4 and rCYP2C8), pooled human liver microsomes (HLM), and NADPH regenerating system were obtained

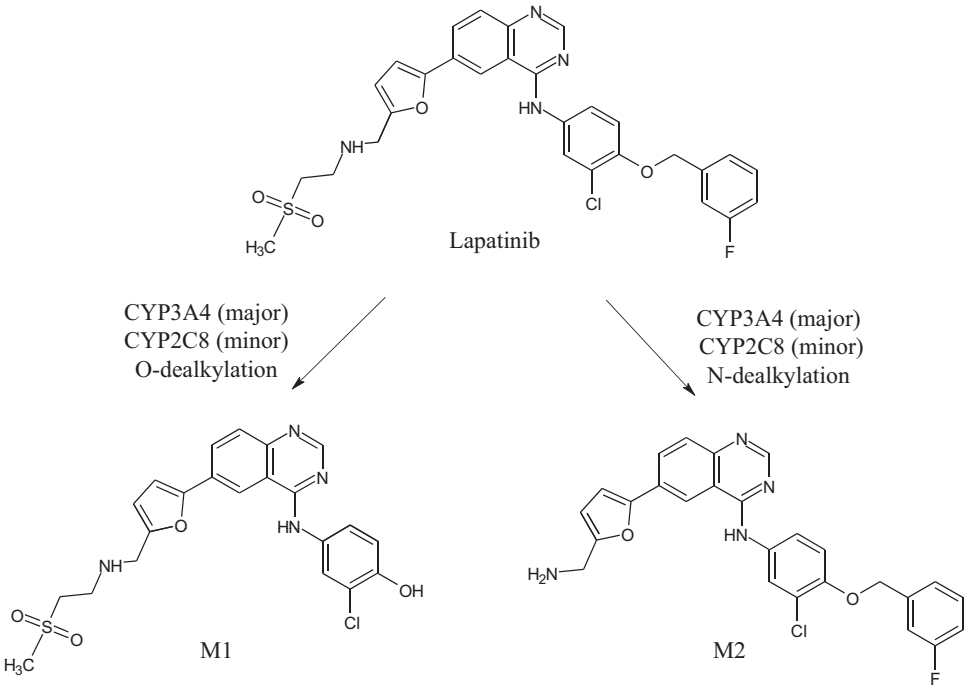


**Fig. 1.** Chemical structures of lapatinib and its two major metabolites, M1 (O-dealkylated lapatinib) and M2 (N-dealkylated lapatinib). The formation of M1 and M2 is mediated by both CYP3A4 (major) and CYP2C8 (minor).

from BD Gentest (Woburn, MA). Water was obtained using a Milli-Q water purification system (Millipore, Billerica, MA). All other reagents used were of analytical grades.

**Time-, Concentration-, and NADPH-Dependent CYP3A4 Inactivation.** Incubations were carried out in 96-well plates. Primary incubations ($n$ = 3) consisting of 0.5 mg/ml HLM, 100 mM potassium phosphate buffer, pH 7.4, NADPH B, and lapatinib (1, 2.5, 5, 10, 20, 40, and 50 $\mu$M) were prepared. After preincubation at 37°C for 6 to 8 min, the reaction was initiated with the addition of NADPH A. The total volume in each well was 160 $\mu$l, and the final organic concentrations in the incubation mixture were 0.1% DMSO and 0.9% ACN (v/v). At 0, 3, 8, 15, 22, and 30 min after the addition of NADPH A, 8 $\mu$l of the primary incubation were transferred to secondary incubation, which contained 200 $\mu$M testosterone (probe substrate), NADPH regenerating system, and 100 mM potassium phosphate buffer, pH 7.4. The total volume of secondary reaction mixture in each well was 160 $\mu$l. The secondary incubation mixtures were further incubated for 10 min at 37°C before 50 $\mu$l aliquots were removed and quenched with an equal volume of ice-cold ACN and 0.008 $\mu$M verapamil (internal standard). In the control incubations, 100 mM potassium phosphate buffer was used in place of NADPH. The same experiment was repeated by replacing lapatinib with erythromycin (1–50 $\mu$M) and ketoconazole (0.05–10 $\mu$M), a known MBI and competitive inhibitor of CYP3A4, respectively. Samples were centrifuged for 16,000$g$ at 4°C for 15 min, and the supernatant was removed for determination of testosterone 6$\beta$-hydroxylation activity by LC/MS/MS. In a separate experiment, rCYP3A4 (20 pmol/ml) replaced HLM. Test compounds (50–500 $\mu$M) were incubated for up to 60 min in the primary incubation.

**Time-, Concentration-, and NADPH-Dependent CYP2C8 Inactivation.** Lapatinib (0.1–10 $\mu$M), gemfibrozil glucuronide, and quercetin (0.1–50 $\mu$M) were prepared in DMSO-acetonitrile [1:1 (v/v)], whereas amodiaquine was dissolved in Milli-Q water. The final acetonitrile and DMSO concentrations were less than 1% and 0.04% (v/v), respectively. To investigate the potential of lapatinib as a CYP2C8 MBI, the two-step incubation scheme described in the CYP3A4 assay was used. Gemfibrozil glucuronide is a known MBI of CYP2C8, whereas quercetin is a known competitive inhibitor. The probe substrate in the secondary incubation was 10 $\mu$M amodiaquine.

**Partition Ratio.** Primary incubations ($n$ = 3) comprising 100 pmol/ml rCYP3A4, NADPH B, lapatinib (1, 1.5, 5, 10, 25, 50 and 75 $\mu$M), and 100 mM potassium phosphate buffer were prepared. After preincubation at 37°C for 6 to 8 min, the reaction was initiated by addition of NADPH A and the mixture was incubated at 37°C for another 45 min, allowing it to go to completion. The total volume in each well was 160 $\mu$l. Eight microliters of the primary incubation was thereafter transferred to the secondary incubation mixture (similar to that prepared for the inactivation studies) and further incubated at 37°C. After 10 min, 50 $\mu$l aliquots were removed and quenched as described. In the negative control, the NADPH regenerating system was replaced with 100 mM potassium phosphate buffer in the primary incubation mixture. The samples were centrifuged for 16,000$g$ at 4°C for 15 min and the supernatant was removed for determination of testosterone 6$\beta$-hydroxylation activity by LC/MS/MS.

**Effect of Exogenous Nucleophiles.** GSH (2 mM) was included in the primary incubation mixture ($n$ = 3) with 0.5 mg/ml HLM, 50 $\mu$M lapatinib, NADPH B, and 100 mM potassium phosphate buffer. The reaction was initiated by addition of NADPH A after preincubation for 6 to 8 min at 37°C to a final volume of 160 $\mu$l. Ten-microliter aliquots were removed at 0, 4, 8, 15, 22, and 30 min and transferred to secondary incubation mixtures for measurement of residual CYP3A4 activity by LC/MS/MS. Negative controls were prepared without both GSH and lapatinib or only without GSH in the primary incubation mixture.

**Substrate Protection.** Excess testosterone (in 1:8 and 1:16 M ratios of lapatinib/testosterone) was added to the primary incubation mixture ($n$ = 3) containing 50 $\mu$M lapatinib, 100 pmol/ml rCYP3A4, NADPH B, and 100 mM potassium phosphate buffer. After preincubation for 6 to 8 min at 37°C, NADPH A was added to initiate the reaction. Aliquots were removed at 0, 3, 8, 15, 22, and 30 min and transferred to secondary incubation mixtures similar to that prepared in the time-dependent inhibition assay, and quantification of 6$\beta$-hydroxytestosterone was determined using LC/MS/MS. Primary reaction mixtures that lacked either testosterone or both lapatinib and testosterone were prepared as negative controls.

**Spectral Difference Scanning.** rCYP3A4 (200 pmol/ml), NADPH regenerating system, and 100 mM potassium phosphate buffer, pH 7.4, were preincubated at 37°C for 6 to 8 min. The reaction was initiated with the addition of 50 $\mu$M lapatinib. The sample mixture was immediately scanned from 400 to 500 nm at 5-min intervals over a 60-min duration using an Infinite M200 Tecan microplate reader (Tecan Group Ltd, Männedorf, Switzerland) that was maintained at 37°C. The spectral differences were obtained by comparing the sample and reference wells (which contained the protein, substrate vehicle, and NADPH). The positive control was prepared using 10 $\mu$M verapamil.

**Reduced CO-Difference Spectroscopy.** Incubations ($n$ = 3) were prepared using 50 $\mu$M lapatinib, NADPH B, and 640 pmol/ml rCYP3A4 in 100 mM potassium phosphate buffer, pH 7.4. After preincubation at 37°C for 6 to 8 min, NADPH A was added to initiate the reaction. The total volume of this mixture was 50 $\mu$l, and it was further incubated at 37°C. At 30 min, the reaction was terminated by the addition of 450 $\mu$l of ice-cold quenching buffer that contained 1 mM EDTA, 20% glycerol, 1% Tergitol NP-40, 2 $\mu$M Safranin O, and 100 mM potassium phosphate buffer, pH 7.4. The resultant mixture was split into two 250 $\mu$l tubes (sample and reference tubes). CO was bubbled into one of the tubes (sample tube) and stopped after approximately 60 bubbles had been passed into the mixture. Approximately 1 mg of sodium dithionite was added to both tubes, and 220 $\mu$l were transferred from each tube into a 96-well plate. The reduced CO-difference spectra for sample and reference wells were acquired by scanning from 400 to 500 nm using a microplate reader (Guengerich et al., 2009). A negative control was prepared by excluding NADPH from the incubation mixture.

**HLM Incubations for Identification of GSH Adducts.** Incubation containing 1 mg/ml HLM, NADPH regenerating system, 100 mM potassium phosphate buffer, pH 7.4, and 50 mM GSH were preincubated at 37°C for 6 to 8 min. The reaction was initiated by the addition of either 5 mM lapatinib or O-dealkylated lapatinib, and the total volume of the incubation mixture was 500 $\mu$l. The final concentration of each substrate was 50 $\mu$M. The synthesis of the O-dealkylated lapatinib metabolite is shown in Supplemental Fig. 1. The final concentrations of organic solvents in the incubation were 0.1% DMSO and 0.9% ACN (v/v). At 60 min, 1 ml of ice-cold ACN was added to quench the reaction. The samples were centrifuged at 16,000$g$ for 15 min at 4°C. Supernatant (1.4 ml) was removed and dried under a gentle flow of nitrogen gas (TurboVap LV; Caliper Life Science, Hopkinton, MA). The samples were reconstituted with 100 $\mu$l of ACN/water [3:7 (v/v)], vortex-mixed, and centrifuged at 16,000$g$ for 15 min. Supernatant (90 $\mu$l) was transferred into the LC/MS/MS vial, and 3 to 5 $\mu$l was injected for LC/MS/MS analysis. Negative controls were prepared by the exclusion of either lapatinib, O-dealkylated lapatinib, NADPH, or GSH in the incubation mixture. In addition, coincubation of lapatinib with 0.2 $\mu$M ketoconazole was performed separately.

**Measurement of Residual CYP3A4 Activity by LC/MS/MS.** The LC/MS/MS system consisted of an ACQUITY UPLC system (Waters, Milford, MA) interfaced with a hybrid quadrupole linear ion-trap mass spectrometer equipped with a TurboIonSpray electrospray ionization (ESI) source (QTRAP 3200; Applied Biosystems, Foster City, CA). The UPLC and QTRAP MS systems were both controlled by Analyst 1.4.2 software (Applied Biosystems). An ACQUITY UPLC BEH C18 column, 1.7 $\mu$m, 50 × 2.1 mm i.d. (Waters), was used to achieve chromatographic separation. The

column and sample temperatures were 45 and 4°C, respectively. The mobile phases used were water with 0.1% formic acid (solvent A) and ACN with 0.1% formic acid (solvent B) delivered at a flow rate of 0.5 ml/min. The elution conditions were as follows: linear gradient 22 to 70% B (0–2.40 min), isocratic at 95% B (2.41–2.99 min), and isocratic at 22% B (3.00–3.50 min). Multiple reaction monitoring transitions of mass-to-charge ($m/z$) ratios from 305 to 269 and from 455 to 165 were carried out in the ESI-positive mode to detect 6$\beta$-hydroxytestosterone and verapamil (internal standard), respectively. The MS source conditions were: curtain gas, 20 psi; collision gas, medium; ionspray voltage, 5500 V; temperature, 550°C; ion source gas 1, 40 psi; and ion source gas 2, 45 psi. The compound-dependent MS parameters for 6$\beta$-hydroxytestosterone were 6, 20, and 3 V for entrance potential (EP), collision energy (CE), and collision cell exit potential (CXP), respectively. For verapamil, the EP, CE and CXP were 7, 37, and 2 V, respectively. The declustering potential and dwell for both 6$\beta$-hydroxytestosterone and verapamil were 52 V and 250 ms, respectively.

**Detection of GSH adducts.** GSH adducts were analyzed using the same LC/MS/MS system as described above. Chromatographic separation was performed on an ACQUITY UPLC BEH C18 column, 1.7 $\mu$m, 100 × 2.1 mm i.d. (Waters). Mobile phases were 0.1% formic acid in water (solvent A) and 0.1% formic acid in acetonitrile (solvent B) delivered at 0.45 ml/min. The elution conditions were: linear gradient 5 to 60% B (0–6.25 min), isocratic at 95% B (6.26–7.09 min), and isocratic at 5% B (7.10–8.00 min). The incubated samples were screened for GSH adducts in both ESI-positive and -negative modes. Precursor ion scan experiments at $m/z$ 272 were performed in the ESI-negative mode. These experiments were used to detect potential GSH adducts in the scan range of $m/z$ 400 to 900 in four mass-to-charge ratio segments. For analyses in ESI-positive mode, neutral loss at $m/z$ 123 was monitored, whereas enhanced product ion scans were performed for all the potential GSH adducts. The MS source conditions were as follows curtain gas, 15 psi; ionspray voltage, 5500 or −4500 V; collision gas, medium; temperature, 550°C; ion source gas 1, 50 psi; and ion source gas 2, 55 psi. The compound-dependent MS parameters were ±75, ±10, ±30 to 40, and ±3 V for declustering potential, EP, CE, and CXP, respectively.

For the accurate mass profiling of the potential GSH adducts, the incubated samples were analyzed using an ACQUITY UPLC system (Waters) interfaced with a quadrupole, orthogonal acceleration time-of-flight tandem mass spectrometer (QTOFMS) equipped with an ESI source (Q-Tof Premier; Waters, Manchester, UK). The UPLC/QTOFMS system was controlled by MassLynx 4.1 software (Waters). Chromatographic separations were performed on an ACQUITY UPLC BEH C18 column, 1.7 $\mu$m, 50 × 2.1 mm i.d. (Waters). The mobile phases, flow rate, and elution conditions were similar to that used for the LC/MS/MS experiments. The QTOFMS system was tuned for optimum sensitivity and resolution in the ESI-positive mode using leucine enkephalin (200 pg/$\mu$l infused at 5 $\mu$l/min). The QTOFMS/MS analysis was operated in the "V" mode, and the optimized conditions were as follows: capillary voltage, 3200 V; sampling cone, 30 V; source temperature, 120°C; desolvation temperature, 350°C; desolvation gas flow, 800 liters/h; collision energy, 10 to 20 eV; MCP detector voltage, 1900 V; pusher voltage, 940 V; pusher voltage offset, −1.00 V; and puller voltage, 725 V. The precursor mass set at $m/z$ of the potential GSH adduct and centroid data were acquired for each sample from 100 to 900 Da with a 0.2-s scan time

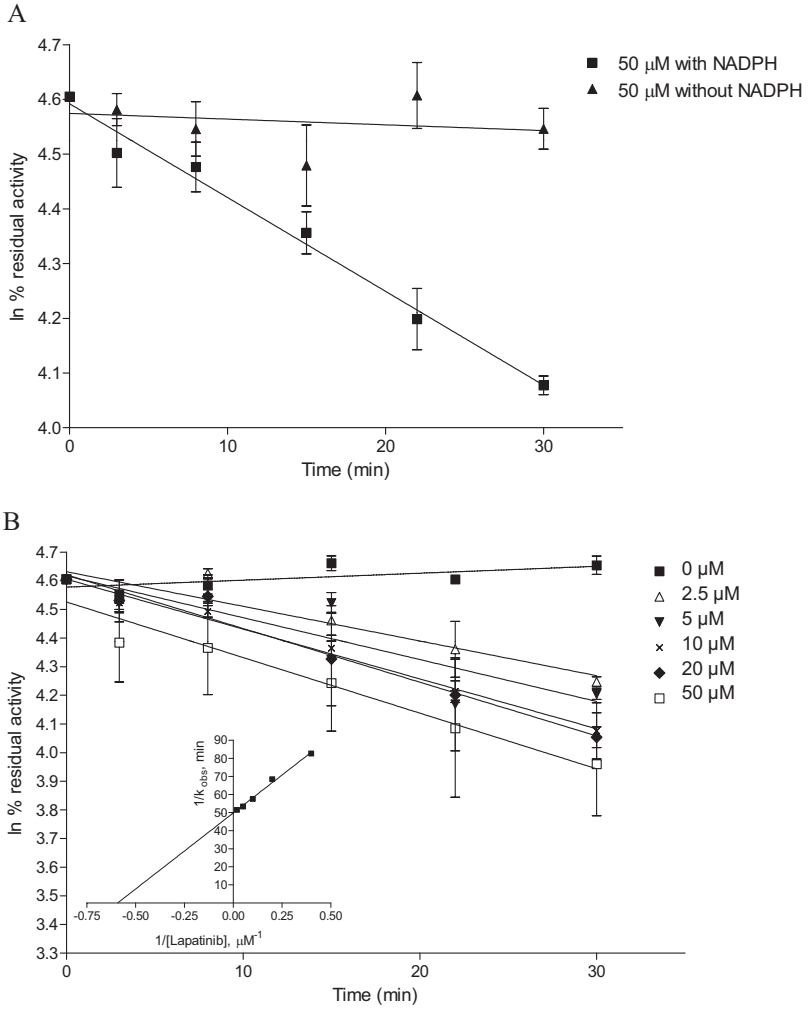


**Fig. 2.** A, NADPH-dependent inactivation of CYP3A4 by lapatinib. Lapatinib (50 $\mu$M) was incubated in the presence and absence of NADPH. B, time- and concentration-dependent inactivation of CYP3A4 by lapatinib. The concentrations of lapatinib used were 0, 2.5, 5, 10, 20, and 50 $\mu$M. The inset shows the Kitz-Wilson plot. Values of $k_{inact}$ and $K_i$ are 0.0202 $min^{-1}$ and 1.709 $\mu$M, respectively. For both plots, each point represents the mean from three replicates with less than 10% S.D.

and a 0.02 s interscan delay. Before analysis, the system was calibrated in the ESI-positive mode using a 0.5 M sodium formate solution infused at a flow rate of 5 μl/min. All analyses were acquired using an independent reference spray via the LockSpray interface to ensure high mass accuracy and reproducibility; the [M+H]+ ion of leucine enkephalin (2 ng/μl infused at 10 μl/min) was used as the reference lock mass ($m/z$ 556.2771). The LockSpray was operated at a reference scan frequency, reference cone voltage, and collision energy of 10 s, 30 V, and 5 eV, respectively.

**Data Analysis.** All chromatographic peak integration was performed using Analyst 1.4.2. To determine the time-, concentration-, and NADPH-dependent activity in the mechanism-based inactivation assays, the mean of triplicate analyses was used to calculate the natural log of percentage probe substrate activity remaining normalized to 0 min against preincubation time. The data were fitted to linear regression and the observed first-order inactivation rate constant, $K_{obs}$, was determined. Kinetic parameters $K_i$ and $k_{inact}$ were determined by a Kitz-Wilson plot (Kitz and Wilson, 1962) to reflect the degree of inactivation of the specific P450 enzyme. These plots were acquired using Prism 4.0 (GraphPad Software, San Diego, CA).

## Results

**Time-, Concentration-, and NADPH-Dependent CYP3A4 Inactivation.** First, we investigated the possible involvement of mechanism-based inactivation of CYP3A4 by lapatinib in preincubations with or without NADPH. Testosterone was used as the substrate, and the formation of testosterone-6β-hydroxylation was used to measure the enzyme activity. Figure 2A shows that lapatinib inhibited CYP3A4 in a NADPH-dependent manner. The absence of NADPH in HLM incubations showed no significant decline in CYP3A4 activity when incubated with lapatinib over the preincubation time of 30 min. On the other hand, the presence of NADPH showed a more pronounced concentration- and time-dependent decrease in CYP3A4 activity. This trend was corroborated with lapatinib in rCYP3A4 incubations for up to 60 min (data not shown).

When HLM were preincubated with lapatinib in the presence of NADPH for up to 30 min, testosterone-6β-hydroxylation activity declined in a time- and concentration-dependent manner (Fig. 2B). Erythromycin (a known MBI of CYP3A4) and lapatinib demonstrated time-dependent decrease of activity with both HLM and rCYP3A4. On the other hand, the negative control, ketoconazole (a potent competitive CYP3A4 inhibitor), showed no preincubation time-dependent decrease in activity. Similar to erythromycin, lapatinib caused a loss in testosterone hydroxylase activity that followed pseudo–first-order kinetics. The kinetic parameters were determined from a Kitz-Wilson plot (Fig. 2B, inset). Lapatinib has been reported previously to be a mixed-competitive inhibitor with $K_i$ of 4 μM (European Medicines Agency, 2008). Under

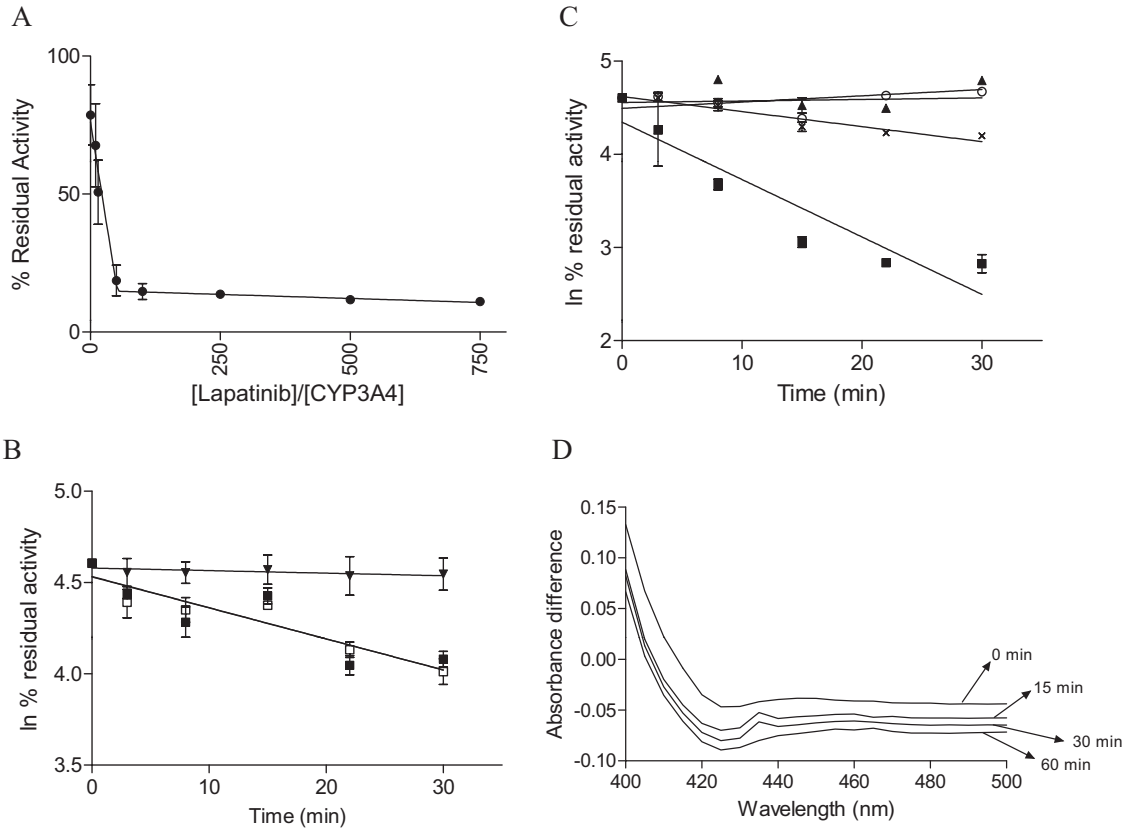


**Fig. 3.** A, determination of the partition ratio for inactivation of CYP3A4 by lapatinib; the estimated partition ratio of 50.9 was determined by extrapolating the intercept of the linear regression line at lower ratios and the straight line for the higher ratios to the $x$-axis. B, effect of GSH on residual CYP3A4 activity. Pooled HLM were incubated with either 2 mM GSH and 50 μM lapatinib (□), 50 μM lapatinib alone (■), or neither lapatinib nor GSH (▼), in the presence of NADPH. C, substrate protection of CYP3A4 with testosterone. rCYP3A4 was incubated with 50 μM lapatinib (■), 1:8 lapatinib/testosterone (○), 1:16 lapatinib/testosterone (▲), and neither lapatinib nor testosterone (×), in the presence of NADPH. D, absorbance difference as a function of wavelength. Lapatinib (50 μM) was incubated with rCYP3A4 in the presence of NADPH. Reference wells contained an equivalent volume of solvent in place of substrate. Spectral differences between sample and reference wells were acquired by scanning from 400 to 500 nm every 5 min for 60 min. For plots A to C, each point represents the mean from three replicates with less than 10% S.D.

our current experimental conditions, the $K_i$ and $k_{inact}$ values of lapatinib were 1.709 $\mu$M and 0.0202 $min^{-1}$, respectively. The $K_i$ and $k_{inact}$ values of erythromycin were 4.579 $\mu$M and 0.0115 $min^{-1}$, respectively. The determined $K_i$ for ketoconazole was 0.177 $\mu$M, which is in the range of reported values of 0.004 to 0.180 $\mu$M (US Food and Drug Administration, 2006).

**Time-, Concentration-, and NADPH-Dependent CYP2C8 Inactivation.** Amodiaquine–N-desethylation activity (a CYP2C8-selective reaction) decreased to 69.89, 59.30, and 71.15% of original activity when HLM were incubated for 30 min in the presence of NADPH with 10 $\mu$M quercetin, gemfibrozil glucuronide, and lapatinib, respectively. The determined $K_i$ for quercetin (competitive inhibitor) and gemfibrozil glucuronide (MBI of CYP2C8) were 0.029 and 0.26 $\mu$M, respectively, whereas the $k_{inact}$ of gemfibrozil glucuronide was 0.015 $min^{-1}$. Lapatinib and the controls exhibited both time- and concentration-

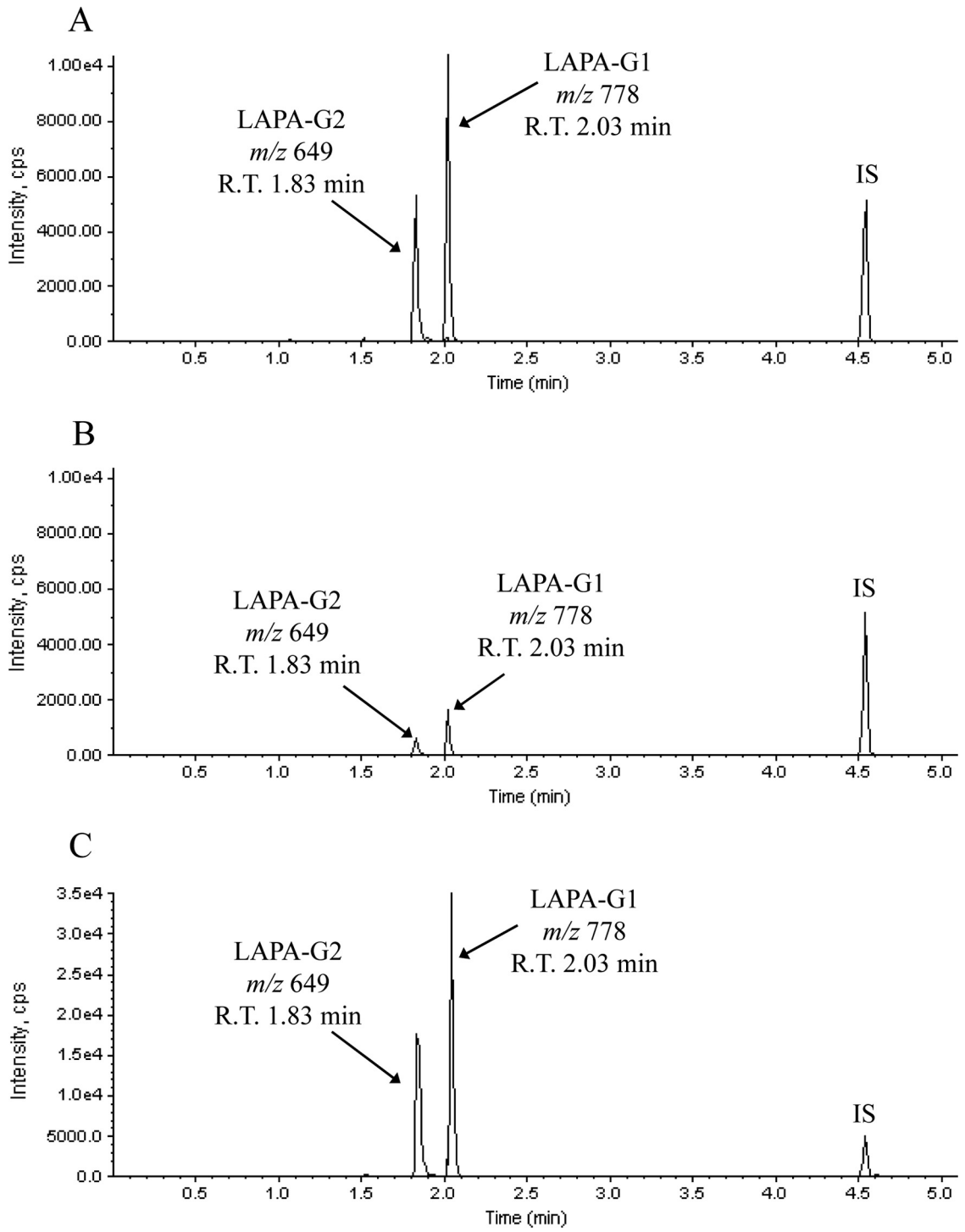


**Fig. 4.** Multiple reaction monitoring chromatograms of HLM incubations with GSH with 50 $\mu$M lapatinib (A), 50 $\mu$M lapatinib and 0.2 $\mu$M ketoconazole (B), and 50 $\mu$M O-dealkylated lapatinib (C). The adducts are labeled as LAPA-G1 and LAPA-G2.

dependent decreases in activity with HLM. However, CYP2C8 inhibition was not increased when HLM were preincubated with quercetin and lapatinib in the presence of NADPH. Conversely, a significant decrease in CYP2C8 activity was observed when gemfibrozil glucuronide was preincubated with HLM plus a NADPH-regenerating system. Hence, our observations suggested that lapatinib is not an MBI of CYP2C8.

**Partition Ratio.** A titration method (Silverman, 1995) was used to determine the partition ratio, which is the number of inactivator molecules metabolized per molecule of enzyme inactivated. Metabolism of lapatinib using rCYP3A4 was performed to completion and 6$\beta$-hydroxytestosterone was used to measure residual CYP3A4 activity. Lapatinib was incubated with rCYP3A4 in the presence of NADPH for 45 min until the reaction was completed. Figure 3A shows the plot of residual CYP3A4 activity versus molar ratios of lapatinib to CYP3A4. Extrapolating the intercept of the linear regression line at lower ratios, and the straight line for the higher ratios to the $x$-axis gave a turnover number of 51.9. Subtracting one from this value yielded a partition ratio of 50.9.

**Effect of Exogenous Nucleophiles and Alternate Substrate on Inactivation.** Addition of GSH (exogenous nucleophile) did not affect the rate of enzyme inactivation. As shown in Fig. 3B, CYP3A4 was inactivated to a similar extent compared with that during incubation with lapatinib alone. Coincubation with 8- and 16-fold excess of testosterone, an alternate substrate of CYP3A4, protected the enzyme from inactivation by lapatinib, as seen in the diminished rate of inactivation with time (Fig. 3C).

**Spectral Difference Scanning.** Metabolite-intermediate complex (MIC)-forming compounds tend to show a characteristic peak in the Soret region (448–458 nm) (Polasek and Miners, 2008). When spectral differences were obtained by scanning from 400 to 500 nm for 60 min, lapatinib showed no observable peak in the Soret region when incubated with CYP3A4 (Fig. 3D), whereas verapamil (a known MIC of CYP3A4) produced a clear peak at 448 to 458 nm (Supplementary Fig. 2).

**Reduced CO-Difference Spectroscopy.** Ferrous (reduced) cytochrome P450 forms a complex with CO to give a spectrally detectable peak at 450 nm. Using the formula for calculating P450 concentration ([$\Delta$A450–$\Delta$A490]/0.091 = nmol of P450 per ml) (Guengerich et al., 2009), the extent of reduction in the 450 nm peak was derived. When 50 $\mu$M lapatinib was incubated with CYP3A4 for 30 min, there was a 43 $\pm$ 7.8% decrease in the peak at 450 nm ($n$ = 3) compared with the control incubation in the absence of NADPH.



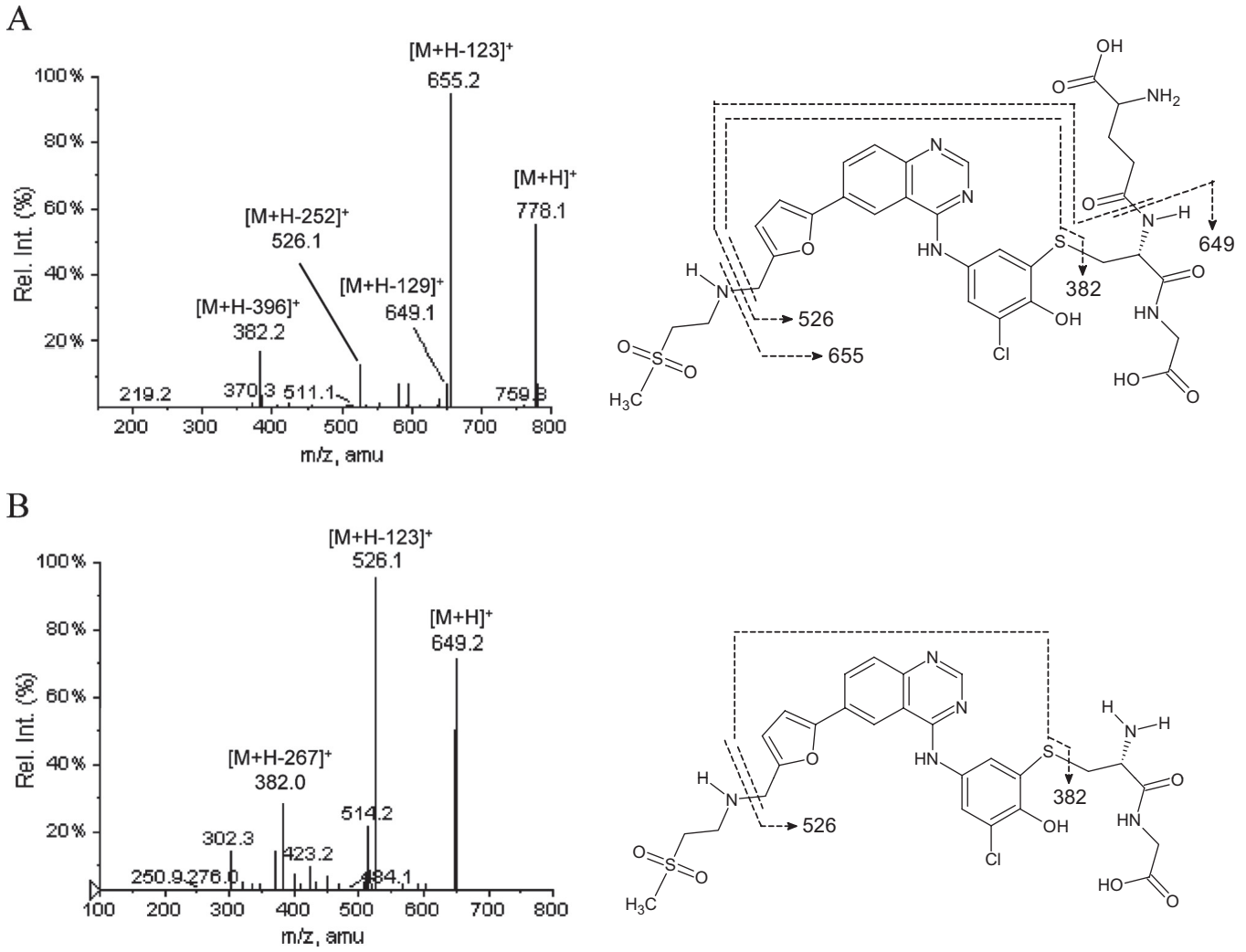


**Fig. 5.** Enhanced product ion scans of LAPA-G1 ($m/z$ 778) (A) and LAPA-G2 ($m/z$ 649) (B).

**Identification of GSH Adducts.** To determine whether generation of RMs was the cause for lapatinib-induced toxicity, GSH-trapping was performed on lapatinib-HLM incubations. Prescreening of GSH-adducts with metabolites of lapatinib were conducted over five separate $m/z$ ranges from $m/z$ 400 to 900 to ensure optimal MS sensitivity. One peak with $m/z$ 778 (LAPA-G1; retention time, 2.03 min) suggestive of a GSH adduct was observed in the precursor scan at $m/z$ 272 in the ESI negative mode and was not observed in any of the negative controls (Fig. 4A). Coincubation with ketoconazole resulted in reduction of the peak (Fig. 4B). The GSH-trapping assay was repeated by incubating O-dealkylated lapatinib in HLM and both LAPA-G1 and LAPA-G2 were also observed in the LC/MS/MS analysis (Fig. 4C).

The enhanced product ion scans of LAPA-G1 (Fig. 5A) generated a spectrum characteristic of collision-induced dissociation fragmentation of GSH where there was a neutral mass loss of 129 corresponding to loss of the pyroglutamic acid moiety. Neutral loss scan at $m/z$ 123 was further performed to profile any additional GSH adducts that shared a fragmentation pattern similar to that of LAPA and a peak at 1.83 min ($m/z$ 649) was detected (Figs. 4 and 5B). To further confirm the identity of the potential GSH adduct, accurate mass measurements were performed using QTOFMS. The program MassLynx was used to determine the potential calculated masses, mass accuracy (mDa and ppm), i-FIT (Norm) (the likelihood that the isotopic pattern of the elemental composition matches a cluster of peaks in the spectrum) values and elemental compositions associated with the measured mass of the GSH adducts and their fragments were generated and summarized in Table 1.

## Discussion

Mechanism-based inactivation of P450 enzymes is preceded by formation of a reactive intermediate and therefore requires NADPH and exhibits both time- and concentration-dependence (Ito et al., 1998). Lapatinib was found to inhibit CYP3A4 in accordance with these criteria with reproducible $K_i$ and $k_{inact}$ values, using a catalytically competent system. We attested the reliability of our data by measuring the $K_i$ and $k_{inact}$ values of the classic CYP3A4 MBI erythromycin and found values consistent with those in the published literature (Table 2). It is noteworthy that the $k_{inact}/K_i$ ratio for lapatinib was lower than that observed for troleandomycin but higher than clinically relevant MBIs such as erythromycin, dihydralazine, and clarithromycin. Erythromycin can cause *torsades de pointes* when coadministered with ter-



TABLE 1
Summarized results of the QTOFMS analyses of the parent and product ions of LAPA-G1 ($m/z$ 778) and LAPA-G2 ($m/z$ 649) using a mass tolerance of 10 ppm

| Chemical Formula | $m/z$ | | mDa | ppm | i-FIT (Norm) |
|---|---|---|---|---|---|
| | Theoretical | Experimental | | | |
| LAPA-G1 | | | | | |
| $C_{32}H_{37}ClN_7O_{10}S_2$ | 778.1732 | 778.1725 | −0.7 | −0.9 | 2.3 |
| $C_{29}H_{28}ClN_6O_8S$ | 655.1378 | 655.1353 | −2.5 | −3.8 | 3.2 |
| $C_{27}H_{30}ClN_6O_7S_2$ | 649.1306 | 649.1308 | 0.2 | 0.3 | 0.9 |
| $C_{24}H_{21}ClN_5O_5S$ | 526.0952 | 526.0944 | −0.8 | −1.5 | 4.2 |
| $C_{19}H_{13}ClN_3O_2S$ | 382.0417 | 382.0410 | −0.7 | −1.8 | 2.3 |
| LAPA-G2 | | | | | |
| $C_{27}H_{30}ClN_6O_7S_2$ | 649.1306 | 649.1302 | −0.4 | −0.6 | 1.9 |
| $C_{24}H_{21}ClN_5O_5S$ | 526.0952 | 526.0939 | −1.3 | −2.5 | 2.5 |
| $C_{19}H_{13}ClN_3O_2S$ | 382.0417 | 382.0414 | −0.3 | −0.8 | 2.1 |

TABLE 2
Comparison of enzyme inactivation kinetic constants for the various mechanism-based inactivators and competitive inhibitor of CYP3A4 using testosterone-6β-hydroxylation as an indication of CYP3A4 residual activity

| Compound & Enzyme Source | $K_i$ | $k_{inact}$ | $k_{inact}/K_i$ | Reference |
|---|---|---|---|---|
| | $\mu M$ | $min^{-1}$ | $min^{-1} \cdot mM^{-1}$ | |
| Ketoconazole | | | | |
| HLM | 0.0037–0.18[a] | | | FDA, 2006 |
| HLM | 0.177[a] | | | In-house data |
| Erythromycin | | | | |
| HLM | 12.8 | 0.037 | 2.891[b] | Polasek and Miners, 2006 |
| rCYP3A4 | 0.92 | 0.058 | 63.043[b] | |
| HLM | 4.579 | 0.0115 | 2.511 | In-house data |
| Lapatinib | | | | |
| HLM | 2.679 | 0.0212 | 7.913 | In-house data |
| Dihydralazine | | | | |
| HLM | 35.0 | 0.0495 | 1.414[b] | Masubuchi and Horie, 1999 |
| Clarithromycin | | | | |
| HLM | 29.5 | 0.050 | 1.695[b] | Polasek and Miners, 2006 |
| rCYP3A4 | 2.25 | 0.040 | 17.778[b] | |
| Mifepristone | | | | |
| rCYP3A4 | 4.7 | 0.089 | 18.936[b] | He et al., 1999 |
| Troleandomycin | | | | |
| HLM | 0.14 | 0.027 | 192.857[b] | Polasek and Miners, 2006 |
| rCYP3A4 | 0.08 | 0.054 | 675.000[b] | |

[a] Ketoconazole is a competitive inhibitor of CYP3A4 but not a mechanism-based inactivator.
[b] Calculated from reported $K_i$ and $k_{inact}$.

fenadine, cisapride, or astemizole and rhabdomyolysis when coadministered with simvastatin (Spinler et al., 1995) through drug-drug interactions. Likewise, dihydralazine had been reported to induce immunoallergic hepatitis (Masubuchi and Horie, 1999). Therefore, it is reasonable to postulate that lapatinib, being an even more potent MBI, may be capable of inducing hepatotoxicity through drug-drug interaction and/or immune-mediated toxicity (Uetrecht, 2007). However, additional clinical data and development of an animal model will be required to determine the exact mechanism of lapatinib-mediated hepatotoxicity.

The efficiency of an MBI is estimated by its partition ratio, which is the number of times each P450 turns over the drug before a reactive intermediate inactivates the enzyme. The measured partition ratio for lapatinib was 50.9, a relatively high value compared with those reported for numerous CYP3A4 MBIs (Ghanbari et al., 2006). Coincubation with GSH did not affect the rate of CYP3A4 inactivation by lapatinib, which suggests that the RM was formed and inactivated by the enzyme before its release from the active site. Coincubation with an alternate substrate, testosterone, protected CYP3A4 from inactivation, further confirming that inactivation by lapatinib occurred at the enzyme's active site. These novel findings collectively substantiated mechanism-based inactivation of CYP3A4 by lapatinib.

At least three mechanisms of inactivation of CYP450 by MBIs have been proposed: alkylation of the P450 heme moiety, modification of P450 apoprotein, and formation of a coordinate covalent bond with the heme iron that results in a MIC (Polasek and Miners, 2007). Spectral analyses were performed to elucidate the mechanistic details of CYP3A4 inactivation by lapatinib. The absence of a Soret peak ruled out the possibility of pseudo-irreversible MIC formation by lapatinib, which suggests that CYP3A4 was irreversibly inactivated by a lapatinib metabolite, most likely via covalent modification of the enzyme. This possibility was supported by reduced CO-difference spectroscopy, which showed a 43% loss of spectrally detectable CYP3A4-CO complex at 450 nm in the presence of lapatinib accompanied by an increase in absorption at 420 nm. Although reduction in absorption at 450 nm could be linked to either heme adduction or heme destruction, covalent adduction of an RM to apoprotein near the heme moiety could compromise the integrity of the CYP3A4 active site. This could thereby interfere with CO-heme binding and lead to an increase in absorption at 420 nm (Omura and Sato, 1964). Covalent adduction to apoprotein has been demonstrated for MBIs such as bergamottin (He et al., 1998) and mifepristone (He et al., 1999), whereas the MBI formed from 17$\alpha$-ethynylestradiol forms adducts to both heme and apoprotein (Lin et al., 2002). Although further work is required to determine how lapatinib inhibits CYP3A4 at the molecular level, we hypothesize that the quinoneimine of the O-dealkylated metabolite of lapatinib binds to the apoprotein of CYP3A4, because it is a relatively soft electrophile that would react with soft nucleophiles on proteins.

The *para*-aminophenol group of the O-dealkylated metabolite of lapatinib (Fig. 1.M1) provided an initial structural alert to its potential toxicity mechanism because it could be oxidized to the reactive quinoneimine species, based on parallels of studies with *N*-acetyl-*p*-benzo-quinoneimine generated from the cytochrome P450 oxidation of acetaminophen (Dahlin et al., 1984; Albano et al., 1985). Moreover, it was confirmed that lapatinib did not inhibit CYP2C8 as an MBI, although it is a competitive inhibitor for this enzyme, which suggests that lapatinib may be metabolized differently or to a different extent by CYP3A4 than by CYP2C8. An RM-GSH

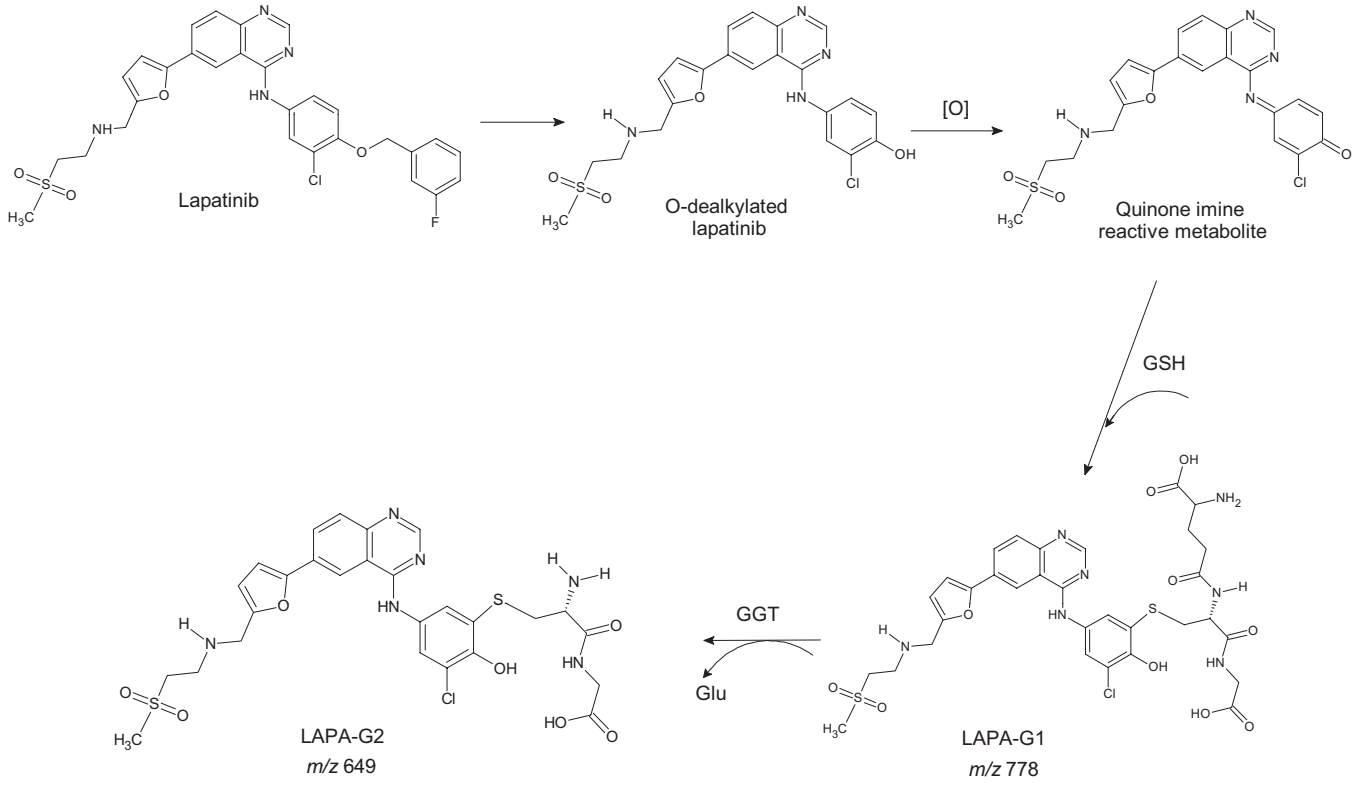


**Fig. 6.** Proposed bioactivation pathway of lapatinib by CYP3A4.

adduct, LAPA-G1, was identified in the present study (Fig. 4). The accurate $m/z$ ratios of the parent and product ions of LAPA-G1 fell within 5 ppm (Table 1A). Coupled to the strong i-FIT values (<5 units) that indicated good fit with the isotopic pattern of each ion, our confidence in the assignment of elemental compositions of the parent and product ions was significantly enhanced. The RM was a quinoneimine generated from the oxidation of the *para*-aminophenol group of the O-dealkylated metabolite (LAPA-G1, $m/z$ 778; Fig. 5A). This was further confirmed by the detection of LAPA-G1 in the incubated sample of O-dealkylated lapatinib with HLM and GSH (Fig. 4C). The proposed bioactivation pathway of lapatinib is summarized in Fig. 6. This bioactivation parallels that of other structurally similar tyrosine kinase inhibitors such as dasatinib (Li et al., 2009) and gefitinib (Li et al., 2009), which have been shown to form similar reactive quinone metabolites and cause idiosyncratic hepatotoxicity. Addition of ketoconazole, a reversible competitive CYP3A4 inhibitor, reduced formation of the RM-GSH adduct in vitro (Fig. 4B), confirming that the RM was generated from oxidative metabolism by CYP3A4.

It is noteworthy that another adduct, LAPA-G2 ($m/z$ 649), was observed and confirmed to be metabolically derived (Fig. 4). Its fragmentation pattern lacked the characteristic neutral loss of 129 associated with a typical RM-GSH adduct (Fig. 5B). It was also noted that the mass difference between LAPA-G1 and -G2 was 129, corresponding to the loss of the pyroglutamic acid moiety of GSH. Furthermore, LAPA-G2 demonstrated fragmentation losses of 123 and a fragment ion at $m/z$ 382, all of which are characteristic of the fragmentation pattern of lapatinib. The accurate $m/z$ ratios of the parent and product ions of LAPA-G2 are within 5 ppm (Table 1B) and low i-FIT values (<3 units). These collectively suggested that LAPA-G2 was a cysteinylglycine conjugate, the secondary metabolite of LAPA-G1 derived from the mercapturate pathway as catalyzed by γ-glutamyltransferase, a human liver microsomal enzyme (Fig. 6). In GSH conjugation of xenobiotics, the mercapturate pathway is a common detoxification route (Stevens, 1989).

Our results raise the possibility that lapatinib-related hepatotoxicity may be an idiosyncratic drug reaction (IDR) that occurs at continuous high dosing. This is in agreement with reports of $C_{max}$ and area-under-the-curve increases that are more than dose-proportional with continuous dosing (European Medicines Agency, 2008). Although IDRs are said to be dose-independent, an apparent dose-response relationship among those at risk may arise from increased cellular protein-RM binding, as demonstrated by the correlation between the risks of IDRs for halogenated anesthetics and the amount of trifluoroacetyl halide RM formed (Njoku et al., 1997). It was observed that drugs administered at less than 10 mg/day are generally rarely associated with IDRs (Uetrecht, 1999), whereas drugs dosed more than 1 g/day (e.g., felbamate) are more likely to cause IDRs (Uetrecht, 2007). Hence, the 1.25 g/day dosing for lapatinib (European Medicines Agency, 2008) could reasonably exceed the threshold level for toxicity in a susceptible subpopulation. Therefore, any involvement of immunohepatotoxicity with lapatinib could not be excluded. In fact, the high therapeutic dose of lapatinib, coupled to its efficiency as a CYP3A4 MBI, could presumably trigger protein modification and immune response, such as with ticrynafen (tienilic acid), which caused rare idiosyncratic hepatotoxicity upon mechanism-based inactivation of CYP2C9, resulting in antibody formation against CYP2C9 (Masubuchi and Horie, 2007). Nevertheless, although IDRs seem to be RM-driven and immune-mediated, host genetic and environmental influences can also be contributory (Uetrecht, 2007). Hence, the clinical characteristics of lapatinib-related hepatotoxicity are crucial in understanding the toxicity mechanism.

In conclusion, we demonstrated for the first time that lapatinib is a CYP3A4 MBI via covalent modification of its apoprotein and/or heme moiety and elucidated the structure of the RM possibly involved in the irreversible inactivation of the enzyme. Future preclinical and clinical studies are needed to further confirm the mechanism of toxicity of lapatinib.

## References


Albano E, Rundgren M, Harvison PJ, Nelson SD, and Moldéus P (1985) Mechanisms of *N*-acetyl-*p*-benzoquinone imine cytotoxicity. *Mol Pharmacol* **28:**306–311.

Dahlin DC, Miwa GT, Lu AY, and Nelson SD (1984) *N*-Acetyl-*p*-benzoquinone imine: a cytochrome P-450-mediated oxidation-product of acetaminophen. *Proc Natl Acad Sci USA* **81:**1327–1331.

European Medicines Agency (2008) Assessment report for Tyverb. Available at: http://www.emea.europa.eu/docs/en_GB/document_library/EPAR_-_Public_assessment_report/human/000795/WC500044960.pdf.

Ghanbari F, Rowland-Yeo K, Bloomer JC, Clarke SE, Lennard MS, Tucker GT, and Rostami-Hodjegan A (2006) A critical evaluation of the experimental design of studies of mechanism based enzyme inhibition, with implications for in vitro-in vivo extrapolation. *Curr Drug Metab* **7:**315–334.

GlaxoSmithKine (2007) Tykerb product information. Available at http://us.gsk.com/products/assets/us_tykerb.pdf.

Gomez HL, Doval DC, Chavez MA, Ang PCS, Aziz Z, Nag S, Ng C, Franco SX, Chow LWC, Arbushites MC, et al. (2008) Efficacy and safety of lapatinib as first-line therapy for ErbB2-amplified locally advanced or metastatic breast cancer. *J Clin Oncol* **26:**2999–3005.

Guengerich FP, Martin MV, Sohl CD, and Cheng Q (2009) Measurement of cytochrome P450 and NADPH-cytochrome P450 reductase. *Nat Protoc* **4:**1245–1251.

He K, Iyer KR, Hayes RN, Sinz MW, Woolf TF, and Hollenberg PF (1998) Inactivation of cytochrome P450 3A4 by bergamottin, a component of grapefruit juice. *Chem Res Toxicol* **11:**252–259.

He K, Woolf TF, and Hollenberg PF (1999) Mechanism-based inactivation of cytochrome P-450–3A4 by mifepristone (RU486). *J Pharmacol Exp Ther* **288:**791–797.

Hinson JA, Pohl LR, and Monks TJ, and Gillette JR (1981) Acetaminophen-induced hepatotoxicity. *Life Sci* **29:**107–116.

Ito K, Iwatsubo T, Kanamitsu S, Ueda K, Suzuki H, and Sugiyama Y (1998) Prediction of pharmacokinetic alterations caused by drug-drug interactions: metabolic interaction in the liver. *Pharmacol Rev* **50:**387–412.

Kitz R and Wilson IB (1962) Esters of methanesulfonic acid as irreversible inhibitors of acetylcholinesterase. *J Biol Chem* **237:**3245–3249.

Li X, He Y, Ruiz CH, Koenig M, and Cameron MD (2009) Characterization of dasatinib and its structural analogs as CYP3A4 mechanism-based inactivators and the proposed bioactivation pathways. *Drug Metab Dispos* **37:**1242–1250.

Li X, Kamenecka TM, and Cameron MD (2009) Bioactivation of the epidermal growth factor receptor inhibitor gefitinib: implications for pulmonary and hepatic toxicities. *Chem Res Toxicol* **22:**1736–1742.

Lin HL, Kent UM, and Hollenberg PF (2002) Mechanism-based inactivation of cytochrome P450 3A4 by 17 alpha-ethynylestradiol: evidence for heme destruction and covalent binding to protein. *J Pharmacol Exp Ther* **301:**160–167.

Masubuchi Y and Horie T (2007) Toxicological significance of mechanism-based inactivation of cytochrome P450 enzymes by drugs. *Crit Rev Toxicol* **37:**389–412.

Masubuchi Y and Horie T (1999) Mechanism-based inactivation of cytochrome P450s 1A2 and 3A4 by dihydralazine in human liver microsomes. *Chem Res Toxicol* **12:**1028–1032.

Medina PJ and Goodin S (2008) Lapatinib: a dual inhibitor of human epidermal growth factor receptor tyrosine kinases. *Clin Ther* **30:**1426–1447.

Nelson MH and Dolder CR (2007) A review of lapatinib ditosylate in the treatment of refractory or advanced breast cancer. *Ther Clin Risk Manage* **3:**665–673.

Njoku D, Laster MJ, Gong DH, Eger EI, Reed GF, and Martin JL (1997) Biotransformation of halothane, enflurane, isoflurane, and desflurane to trifluoroacetylated liver proteins: association between protein acylation and hepatic injury. *Anesth Analg* **84:**173–178.

Omura T and Sato R (1964) Isolation of cytochromes P-450 and P-420. *Methods Enzymol* **239:**101819.

Park KB, Dalton-Brown E, Hirst C, and Williams DP (2006) Selection of new chemical entities with decreased potential for adverse drug reactions. *Eur J Pharmacol* **549:**1–8.

Polasek TM and Miners JO (2006) Quantitative prediction of macrolide drug-drug interaction potential from in vitro studies using testosterone as the human cytochrome P4503A substrate. *Eur J Clin Pharmacol* **62:**203–208.

Polasek TM and Miners JO (2007) In vitro approaches to investigate mechanism-based inactivation of CYP enzymes. *Expert Opin Drug Metab Toxicol* **3:**321–329.

Polasek TM and Miners JO (2008) Time-dependent inhibition of human drug me-

tabolizing cytochromes P450 by tricyclic antidepressants. *Br J Clin Pharmacol* **65:**87–97.
Rock D, Schrag M, and Wienkers LC (2009) Experimental characterization of cytochrome P450 mechanism based inhibition, in *Handbook of Drug Metabolism* (Pearson PG, Wienkers LC eds) pp 541–569, Informa HealthCare, UK.
Rusnak DW, Affleck K, Cockerill SG, Stubberfield C, Harris R, Page M, Smith KJ, Guntrip SB, Carter MC, Shaw RJ, et al. (2001) The characterization of novel, dual ErbB-2/EGFR, tyrosine kinase inhibitors: potential therapy for cancer. *Cancer Res* **61:**7196–7203.
Ryan Q, Ibrahim A, Cohen MH, Johnson J, Ko CW, Sridhara R, Justice R, and Pazdur R (2008) FDA drug approval summary: lapatinib in combination with capecitabine for previously treated metastatic breast cancer that overexpresses HER-2. *Oncologist* **13:**1114–1119.
Silverman RB (1995) Mechanism-based enzyme inactivators. *Methods Enzymol* **249:** 240–283.
Spinler SA, Cheng JW, Kindwall KE, and Charland SL (1995) Possible inhibition of hepatic metabolism of quinidine by erythromycin. *Clin Pharmacol Ther* **57:**89–94.
Stevens JL (1989) The mercapturic acid pathway—biosynthesis, intermediary metabolism, and physiological disposition, in *Glutathione: Chemical, Biochemical, and Medical Aspects* (Dolphin D, Avramović O, Poulson R eds) pp 46–84, John Wiley and Sons, New York.
US Food and Drug Administration (2006) Drug development and drug interactions: table of substrates, inhibitors and inducers. Available at: http://www.fda.gov/Drugs/DevelopmentApprovalProcess/DevelopmentResources/DrugInteractionsLabeling/ucm081177.htm.
Uetrecht JP (1999) New concepts in immunology relevant to idiosyncratic drug reactions: the "danger hypothesis" and innate immune system. *Chem Res Toxicol* **12:**387–395.
Uetrecht JP (2007) Idiosyncratic drug reactions: current understanding. *Annu Rev Pharmacol Toxicol* **47:**513–539.
Xia W, Mullin RJ, Keith BR, Liu LH, Ma H, Rusnak DW, Owens G, Alligood KJ, and Spector NL (2002) Anti-tumor activity of GW572016: a dual tyrosine kinase inhibitor blocks EGF activation of EGFR/erbB2 and downstream Erk1/2 and AKT pathways. *Oncogene* **21:**6255–6263.

**Address correspondence to:** Address correspondence to: Eric C. Y. Chan, Department of Pharmacy, Faculty of Science, National University of Singapore, 18 Science Drive 4, Singapore 117543, Singapore. E-mail: phaccye@nus.edu.sg